Marine Micropaleontology, 8 (1983/84) 261—281
Elsevier Science Publishers B.V., Amsterdam — Printed in The Netherlands

LATE MIOCENE MAGNETOBIOSTRATIGRAPHY OF CRETE

C.G. LANGEREIS[1], W.J. ZACHARIASSE[2] and J.D.A. ZIJDERVELD[1]

[1] *Paleomagnetisch Laboratorium, Fort Hoofddijk, Budapestlaan 17, 3584 CD Utrecht (The Netherlands)*
[2] *Instituut voor Aardwetenschappen, Budapestlaan 4, 3584 CD Utrecht (The Netherlands)*

(Received May 25, 1983; revised version accepted October 6, 1983)

Abstract

Langereis, C.G., Zachariasse, W.J. and Zijderveld, J.D.A., 1984. Late Miocene magnetobiostratigraphy of Crete. Mar. Micropaleontol., 8: 261—281.

Six Upper Miocene marine clay sections on Crete (Greece) have been subjected to a detailed magnetobiostratigraphic analysis. Six correlatable polarity zones are recognized and these demonstrate the regional synchrony of planktonic foraminiferal biohorizons.

By way of correlation to the magnetic polarity time-scale of Lowrie and Alvarez (1981), the Cretan sequence is assigned to polarity chronozones 5 (anomaly 3A) and 6. The new chronology provides an age of 5.6 Ma for the first occurrence datum (FOD) of the *Globorotalia conomiozea* group in the Mediterranean, an age of 6.0 Ma for the FOD of *G. menardii* form 5 and an age of 6.6 Ma for the last occurrence datum (LOD) of *G. menardii* form 4.

Correlating the polarity record of the New Zealand Blind River section (Kennett and Watkins, 1974), with the magnetic polarity time-scale provides an age of 6.0 Ma for the evolutionary appearance of *Globorotalia conomiozea*, which is in complete agreement with the age of 6.1 ± 0.1 Ma given by Loutit and Kennett (1979). The demonstrated diachrony of 0.4 Ma between the New Zealand FOD of *G. conomiozea* and its Mediterranean counterpart is explicable in view of the different nature of the two events, the one in New Zealand being evolutionary and the one in the Mediterranean migrational.

The FOD of the *G. conomiozea* group in the Tortonian/Messinian boundary stratotype section coincides with the level proposed by Colalongo et al. (1979) to mark the base of the Messinian. Since the FOD of the *G. conomiozea* group in Crete and in Sicily are most probably time-equivalent, the age of the Tortonian/Messinian boundary is fixed at 5.6 Ma.

The youngest sediments incorporated in this study extend into the Gilbert chronozone and antedate the main evaporitic phase. Consequently, the Messinian evaporitic body is younger than the base of the Gilbert chronozone, the age of which is fixed at 5.3 Ma. Adopting an age of 5.0 Ma for the Miocene/Pliocene boundary would imply that evaporites and post-evaporitic Lago Mare sediments were deposited in some 300,000 years and suggests that in the central parts of the Mediterranean basins evaporites must have accumulated at rates of some 3 m per 1000 years.

Introduction

As part of IGCP-project "Accuracy in time" a magnetostratigraphic study was initiated to find out whether it would be possible to design a detailed geomagnetic polarity stratigraphy for the Upper Miocene of Crete.

Crete was chosen because we had detailed information about the Neogene sedimentary-tectonic history (Freudenthal, 1969; Meulenkamp, 1969, 1979a, b; Meulenkamp et al., 1979), and because a great number of well exposed marine clay sections and a detailed biostratigraphy were available (e.g. Sissingh, 1972; Schmidt, 1973; Zachariasse, 1975).

Initial sampling and measurements were focused on two Tortonian/Messinian clay sections in western Crete (sections Potamida

0377-8398/84/$03.00

1 and 2), the results of which were published earlier along with detailed micropaleontological analyses (Langereis and Zijderveld, 1979; Langereis, 1979, Drooger et al., 1979a). Later, more sections were sampled from western and central Crete in order to check the initial results and to extend the stratigraphic range of the initial polarity reversal sequences. Stratigraphic positioning of the sections is based mainly on biostratigraphic correlations and to a lesser degree on lithostratigraphic evidence. Part of the results of this enlarged collection of samples are presented here and include a detailed polarity stratigraphy for the Upper Miocene of Crete.

Although a polarity stratigraphy consists of a non-ordinal repetition of polarity reversals, differences in the duration of individual polarity zones make polarity reversal sequences applicable for time-stratigraphic correlations, provided accumulation rates in sections to be correlated are more or less uniform and independent stratigraphic control (i.e. biostratigraphy, radiometric dating) is available. For the Cretan polarity reversal sequences these conditions are fulfilled through which it is possible to calibrate these sequences correctly to the magnetic polarity time-scale based on sea floor anomalies. In this study the most recent magnetic time-scale is employed (Lowrie and Alvarez, 1981).

Sections and sampling

The study reported here is based on six sections. Five of them are located in western Crete, near the villages of Potamida (sections Potamida 1, 2, 3, 4) and Skouloudhiana (section Skouloudhiana) and one section is located in central Crete near the village of Kastelli (section Kastelli) (Fig. 1).

The sections from western Crete consist of open-marine, blue-grey, homogeneous clays which form the upper part of a clastic sediment succession that unconformably overlies pre-Neogene rocks. These clastic sediments are of Tortonian to earliest Messinian Age. Fine-clastic Upper Tortonian sediments were deposited in the more central parts of various subbasins, whereas coarse-clastic sediments and bioclastic limestones accumulated along the margins and on or along submarine ridges (Meulenkamp, 1979a). The blue-grey, homogeneous clays of western Crete are overlain by alternating homogeneous and laminated, beige to whitish marls of Messinian Age.

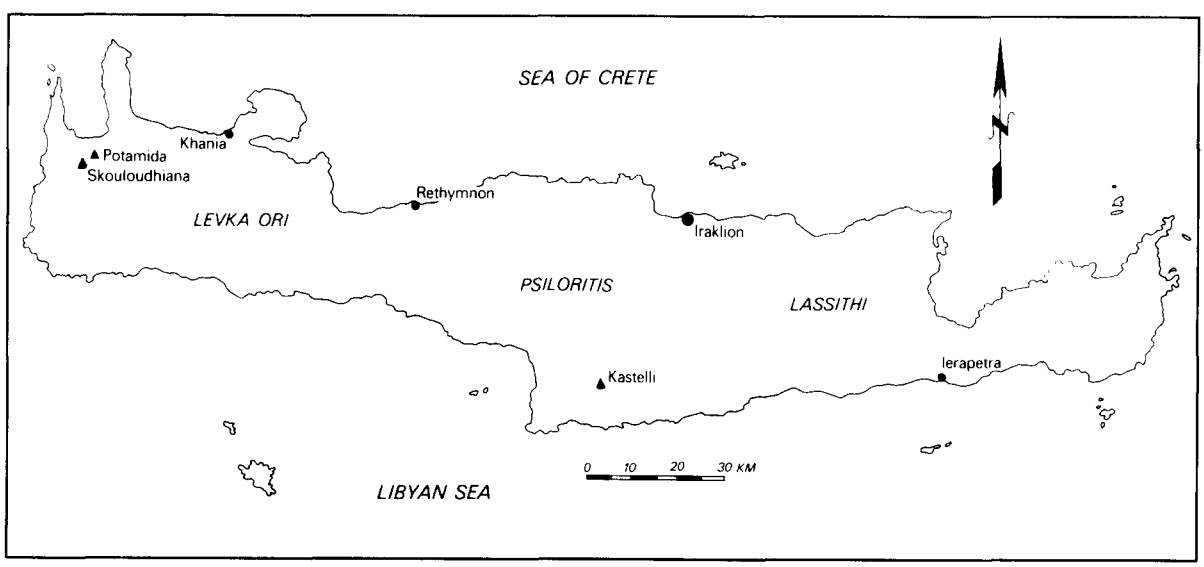

Fig. 1. Location of Cretan sections.

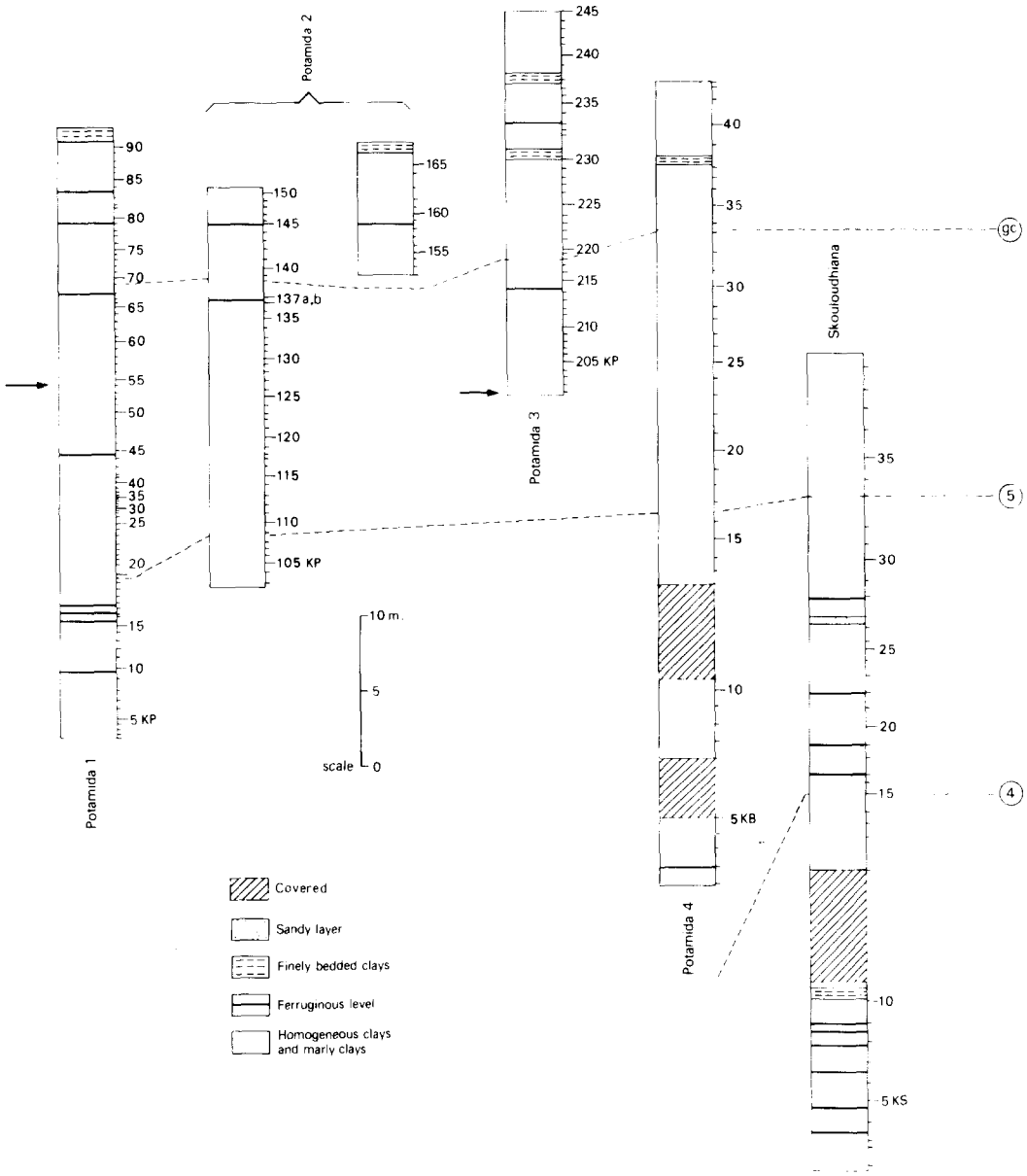

Fig. 2. Western Cretan sections showing lithology and position of paleomagnetic samples. *gc* = FOD of the *G. conomiozea* group; *5* = FOD of *G. menardii* form 5; *4* = LOD of *G. menardii* form 4. Arrow indicates re-appearance level of sinistrally keeled globorotaliids.

Section Kastelli from central Crete is composed of open-marine, blue-grey homogeneous clays with some sandy interbeds. This succession overlies a rapidly alternating sequence of marine, brackish and lacustrine sediments of Early Tortonian Age. Upwards, the open marine clays are replaced by an alternating homogeneous-laminated marl succession, which in turn is overlain by a thick sequence of evaporites (Meulenkamp et al., 1979).

The lithology of the sections, the position of paleomagnetic samples and the biohorizons are shown in Fig. 2. Paleontological samples

were taken at each paleomagnetic sample level in all sections except in Potamida 1 and 2, where they were taken independently and calibrated afterwards (Langereis and Meulenkamp, 1979). It should be noted that the ferruginous levels indicated in Fig. 2 represent thin sandy, iron-rich turbidites and do not correspond to sedimentary hiatuses (Drooger et al., 1979b).

Sections Potamida 1, 2 and 3 were sampled at close intervals (40—55 cm); in sections Potamida 4 and Skouloudhiana a wider spacing was used (120—140 cm). In the Kastelli section samples were taken at intervals of 70—80 cm. At each level three or four cores of 25 mm diameter were taken with an electric drill using water under pressure as coolant. A portable generator was used as power supply. In the paleomagnetic laboratory "Fort Hoofddijk" the cores were divided into specimens 22 mm long, yielding one to four specimens per core.

Stratigraphic distance between sampling levels was determined accurately using vertical and horizontal distance and azimuth between sites as well as strike and dip of the bedding plane (Langereis and Meulenkamp, 1979). For the sections Potamida 4 and Skouloudhiana a theodolite was used to determine the stratigraphic thickness of the whole section as a check on the total of the inter-sample distances.

Biostratigraphy

Selection and stratigraphic ordering of the sections used for designing a detailed polarity stratigraphy for the Upper Miocene of Crete is based mainly on biostratigraphic correlations.

Intra-Mediterranean biostratigraphic control in the Upper Miocene is rather poor, compared to the Middle Miocene and Pliocene. Commonly three planktonic foraminiferal biohorizons are used to subdivide the Mediterranean Upper Miocene. The FOD of *Neogloboquadrina acostaensis* corresponds with a level slightly above the base of the Tortonian and the FOD of *Globorotalia conomiozea* is currently used to recognize the base of the Messinian (D'Onofrio et al., 1975; Colalongo et al., 1979). In a strict sense the FOD of *Globorotalia conomiozea* refers to the first occurrence of *G. conomiozea* types in the Mediterranean. More broadly interpreted this biostratigraphic event corresponds to the sudden spreading of left-coiled, planoconvex, keeled globorotaliids having on the average 4.5 crescent-shaped chambers (Zachariasse, 1979a, b). This group of globorotaliids is labelled here and earlier as the *Globorotalia conomiozea* group and encloses, in addition to the high-conical *Globorotalia conomiozea* type, such forms as the low-convex *G. miotumida* type and the 5—6 chambered *G. mediterranea* type.

Relative to the entry level of the calcareous nannoplankton taxon *Reticulofenestra rotaria* (Theodoridis, 1983) the FOD of the *Globorotalia conomiozea* types, however, fluctuates and is either coeval or to a certain extent younger than the FOD of the *G. conomiozea* group.

The sudden spreading of the *Globorotalia conomiozea* group in the Mediterranean most probably represents a migrational event (Zachariasse, 1979a, b; Wernli, 1980) and constitutes a definite marker level in Late Miocene Mediterranean biostratigraphy.

The youngest biostratigraphic event in the Mediterranean Upper Miocene is a shift, from sinistral to dextral, in the coiling of *Neogloboquadrina acostaensis* which occurs somewhere in the Messinian close to the beginning of the main evaporitic phase.

Because the stratigraphic position of all sections is well above the FOD of *Neogloboquadrina acostaensis* and definitely below the coiling shift of *N. acostaensis*, the entry level of the *Globorotalia conomiozea* group would seem the only distinct biohorizon available for correlating the sections. Fortunately, the discontinuous distribution and coiling changes in keeled globorotaliids other than the *Globorotalia conomiozea* group can also be used for biostratigraphic control.

Generally, keeled globorotaliids occur in low frequencies and are distributed rather discontinuously in the Mediterranean Upper

Miocene. Sinistral assemblages disappear somewhere in the Tortonian and, following a prolonged period of absence of keeled globorotaliids, dextral assemblages reappear in the record. The sinistral and dextral assemblages have been labelled as *Globorotalia menardii* form 4 and as *G. menardii* form 5, respectively (Tjalsma, 1971; Zachariasse, 1975, 1979a, b). In the Mediterranean this pattern is very consistent and allows for a subdivision of the Upper Tortonian into a lower zone with sinistral assemblages, an upper zone with dextral assemblages and an intermediate zone in which keeled globorotaliids are absent for a prolonged period.

The abrupt and instantaneous recurrence of sinistrally keeled globorotaliids above the FOD of *Globorotalia menardii* form 5, recorded in sections Potamida 1 and 3 (Figs. 2, 12), is troublesome for the positioning of single assemblages of keeled globorotaliids but useful for the positioning of sample series. These sinistrally keeled globorotaliids are biometrically intermediate between *Globorotalia menardii* form 4 and *G. menardii* form 5 and the *G. conomiozea* group. In Fig. 14 the generalized distribution pattern of all keeled globorotaliids in the Upper Tortonian/Lower Messinian of Crete is shown and tied to the Cretan polarity stratigraphy.

Laboratory treatment of paleomagnetic samples

The total natural remanent magnetization (total NRM) of (initially) one specimen per core was measured on a ScT cryogenic magnetometer or a JR-3 spinner magnetometer. As an example of the directions of the total NRM, the results for section Potamida 1 are shown in Fig. 3. Reversed polarities are clearly present, but a further analysis of the total NRM is necessary to remove recent normal polarity overprinting and to arrive at a reliable polarity reversal pattern. Since the total NRM-intensity may represent the resultant vector of two or more magnetizations,

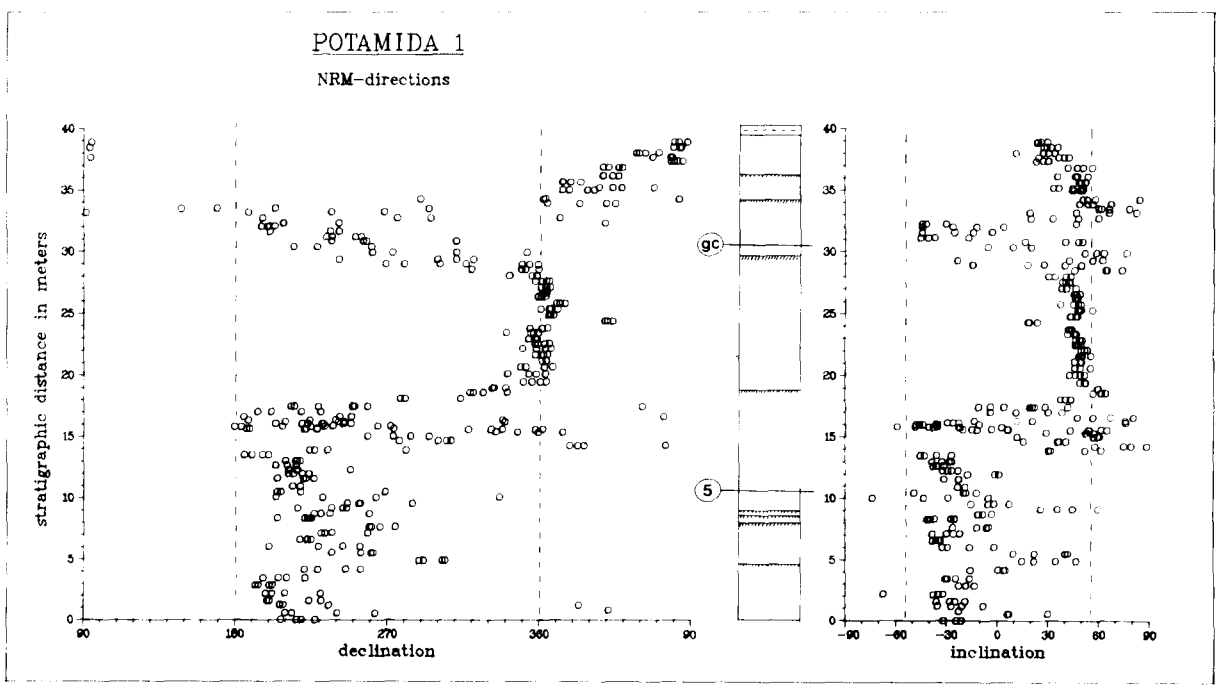

Fig. 3. Declination and inclination of the total NRM in section Potamida 1. Dashed lines represent declination and inclination of the geocentric axial dipole field.

intensity values allow for preliminary conclusions only. In general the total NRM-intensities of the clays vary from 1 to 20 mA m^{-1}. In the uppermost part of Potamida 3 and 4, above the (lower) layer of finely-bedded clay (Fig. 2), total NRM intensities are lower: 0.1—1.0 mA m^{-1} (Fig. 4). The intensity variations are matched by variations in susceptibility and saturation isothermal remanent magnetization (SIRM), suggesting that lithology is responsible for these lower values. In many cases a decrease in intensity is found close to the ferruginous levels (Fig. 4). Remanent coercive forces and saturation remanences of the samples close to these levels indicate oxydation of the original magnetic minerals. Since these ferruginous, sandy levels are more permeable than the dense clay, oxidation and the resultant drop in intensity are most probably induced by weathering.

At least one specimen per core has been demagnetized progressively, either in alternating fields increased stepwise up to a maximum of 200 mT (2000 Oe) peak value or by stepwise heating of the samples in a non-magnetic furnace up to temperatures of 600—650°C. In many cases the samples contained small, randomly directed components, apparently acquired in the laboratory. These viscous components were removed in a peak field of 5—10 mT or at temperatures of 100—110°C (Fig. 5). Secondary normal polarity components with a steep present-day inclination are most probably of recent origin and were removed in a peak field of 50—60 mT; often these components could be completely removed by thermal demagnetization at temperatures as high as 500°C (Fig. 5). A stable and characteristic magnetization component can be determined by stepwise demagnetization in peak fields from 50—60 mT up to 100—200 mT or by thermal demagnetization at temperatures of 500°C and higher. Thermal demagnetization shows that the characteristic remanent magnetization (ChRM) resides mainly in magnetite, since

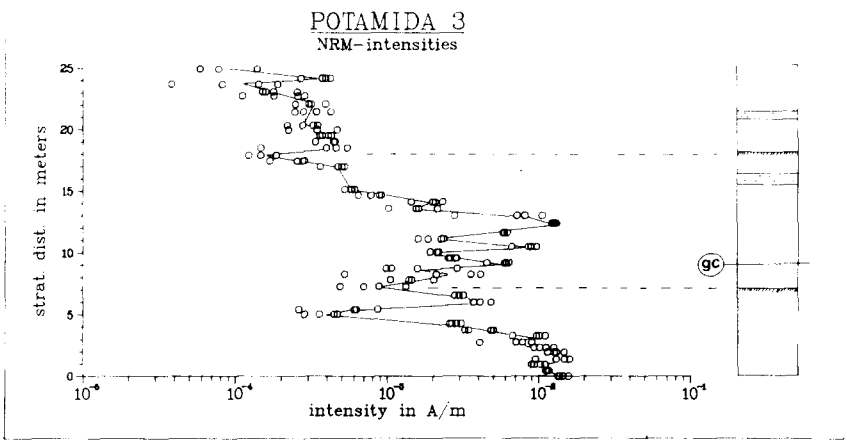

Fig. 4. Total NRM-intensities in section Potamida 3. Solid line represents average intensity. Dashed lines indicate lowered intensity related to ferruginous levels.

Fig. 5. Representative demagnetization vector diagrams of selected samples. Alternating field demagnetizations are given in the left-hand diagrams; thermal demagnetizations of specimens from the same core or same sample level are represented in the right-hand diagrams. Generally thermal demagnetization produces more consistent results (e.g., KB 32) and sometimes displays a reversed ChRM, whereas alternating field demagnetization shows normal polarities (e.g., KT 56). Solid (open) circles denote projection of end points of remanent magnetization vectors on the horizontal (vertical) plane. Numbers refer to peak field in millitesla (mT) or temperature in degrees Celsius.

KP 61 2A

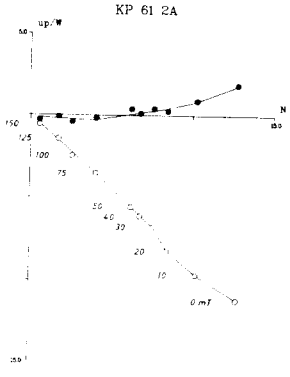

KP 61 3B

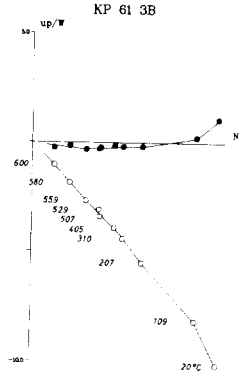

KP 130 3A

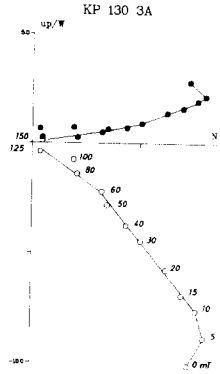

KP 130 3B

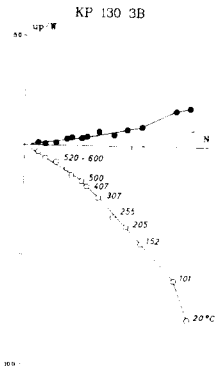

KP 208 3A

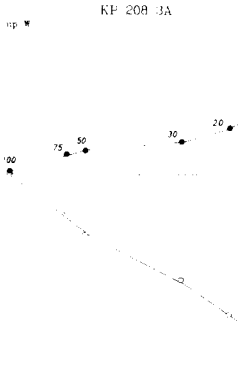

KP 208 4A

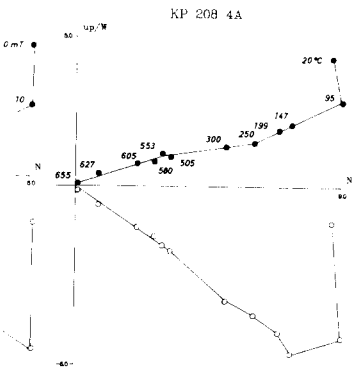

KS 26 2B

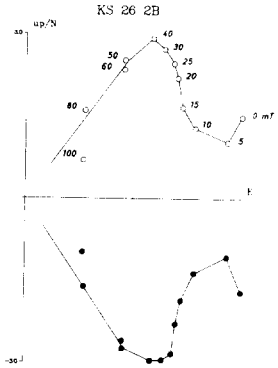

KS 26 3A

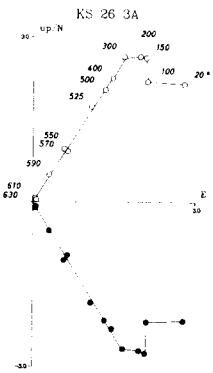

KB 16 3B

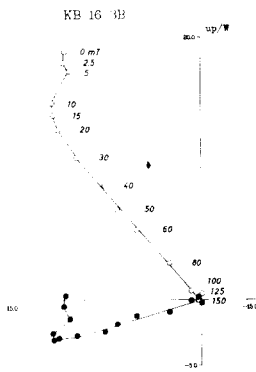

KB 16 3A

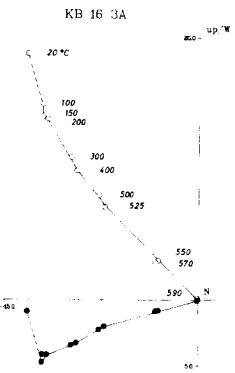

KB 32 3B

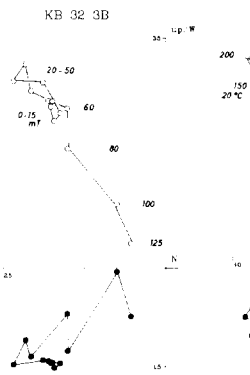

KB 32 3A

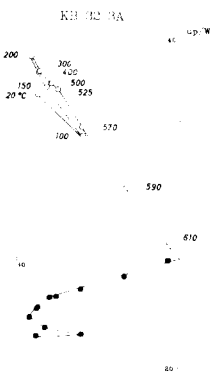

KT 27 2A

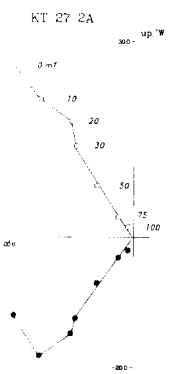

KT 27 3A

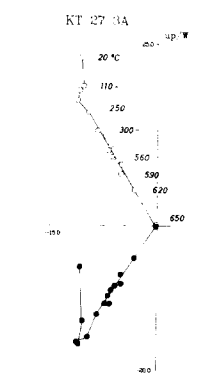

KT 56 1

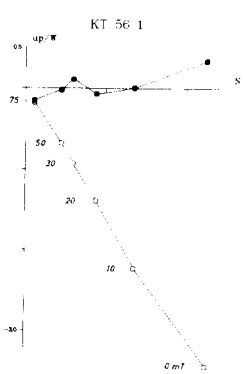

KT 56 3A

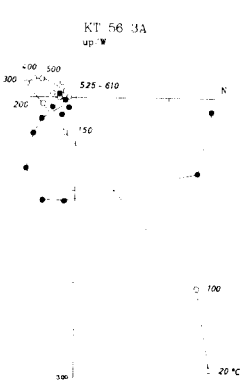

units in mA/m

most of the total NRM was removed at temperatures of ca. 590°C (e.g., KP 130 3A; KB 16 3A in Fig. 5). Some hematite is often present and the remanence is then completely removed at temperatures of 610—650°C (e.g., KP 208 4A; KT 27 3A in Fig. 5).

Although directions of the ChRM derived from alternating field and thermal demagnetization diagrams are generally shown to agree very well (Fig. 5; Langereis, 1979), results derived from thermal demagnetization are often more consistent and the characteristic directions can be determined more accurately (e.g., KB 32 in Fig. 5). Especially in section Kastelli thermal demagnetization sometimes revealed clearly reversed polarities, whereas alternating field demagnetization showed normal polarities (e.g., KT 56 in Fig. 5). Obviously the coercive spectra of the secondary and characteristic magnetizations did overlap, but the blocking temperature spectra overlapped only partially.

Paleomagnetic results

The ChRM-directions of the Cretan sections derived from progressive stepwise demagnetizations are shown in Figs. 6—11. In general, ChRM-directions vary little per sample level. Largest differences occur in the top part of the sections and close to lithological discontinuities and are thought to be induced by weathering processes.

The recorded deviations in the declination of the ChRM from the geocentric axial dipole field may be due to depositional processes (e.g., sediment transport) or to local tectonics. The shallower inclinations are incompatible with the geocentric axial dipole field; this may be due to an inclination error (King, 1955), to compaction of the clays (Valente et al., 1982) and/or to a northward displacement of Crete since the Late Miocene. The existence of an excentric dipole field during the Tertiary cannot be ruled out either (Wilson, 1971).

Fig. 6 shows the ChRM-directions and polarity zones in section Potamida 1. A long, reversed polarity zone (C—) in the lower part of the section is followed upwards by polarity zones D+, E— and F+. The same four polarity zones can be recognized in section Potamida 2 (Fig. 7) on the basis of biostratigraphic evidence. The strongly reduced thickness of polarity zone F+ relative to that measured in section Potamida 1 is due to faulting which caused a doubling in the polarity pattern of section Potamida 2 (Langereis, 1979; Drooger et al., 1979b).

Section Potamida 3 was sampled to establish the upper boundary of polarity zone F+. As shown in Fig. 8, the lower reversed polarity interval is biostratigraphically correlatable with polarity zone E—. Since the uppermost part of section Potamida 3 shows reversed polarities, polarity zone F+ is well defined. Polarity zone G— represents the highest magnetostratigraphic unit recorded in western Crete. The alternating homogeneous-laminated marl sequence overlying section Potamida 3 shows considerable (normal) overprinting, and intensities of the ChRM are far too low.

The reversed polarity zone in the lower half of section Potamida 4 correlates with polarity zone C— (Fig. 9). The true thickness of zone C—, however, is uncertain due to possible faulting in the interval corresponding to the upper gap in the sample record (Fig. 10). The thickness of polarity zone E— is notably reduced relative to that measured in the other Potamida sections. Moreover, the FOD of the *Globorotalia conomiozea* group coincides exactly with the boundary between polarity zones E— and F+, which is also anomalous relative to the position of the FOD in the other sections. On revisiting the section we found that polarity zone E— is reduced tectonically in thickness due to faulting.

Biostratigraphic evidence indicates that section Skouloudhiana extends to much older levels than do the Potamida sections. The base of the section contains the lowermost marine clay levels we could sample in NW Crete. As shown in Fig. 10, the upper reversed polarity zone correlates with zone C—. Downwards, at least four polarity zones are added to the existing polarity reversal sequence. Amongst these four, polarity zones

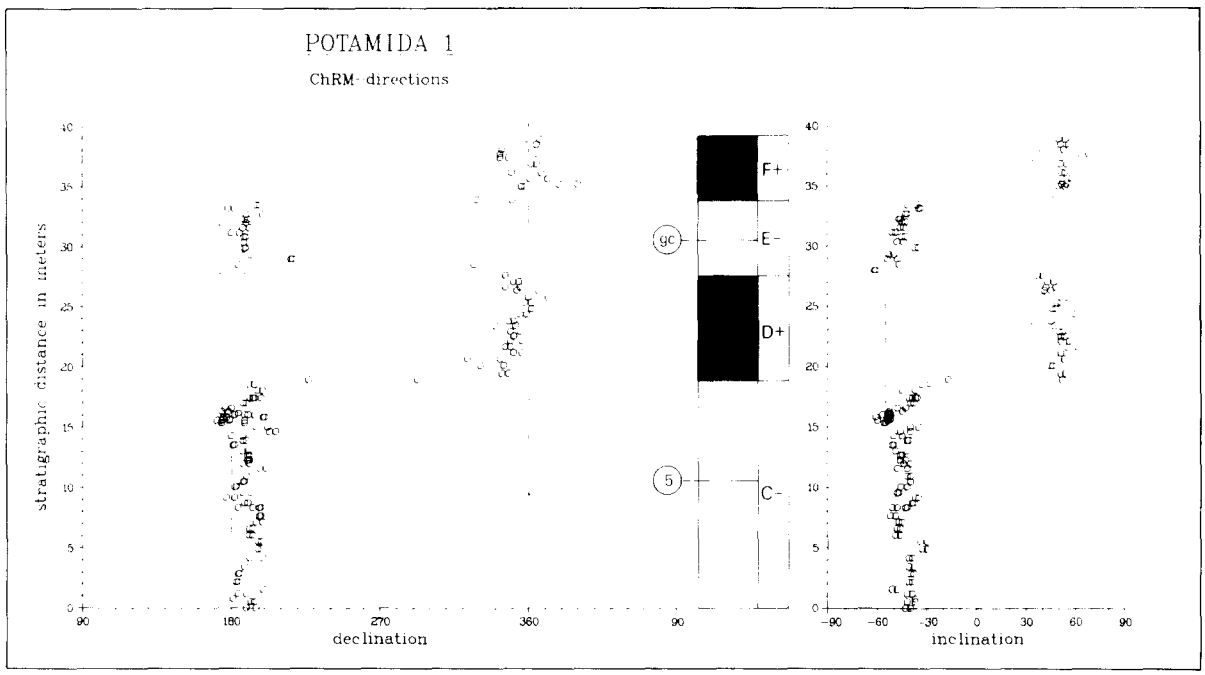

Fig. 6. Declination and inclination of ChRM in section Potamida 1. Black (white) intervals represent normal (reversed) polarities. Dashed lines indicate declination and inclination of the geocentric axial dipole field for the present latitude of the locality. Polarity zones are labelled with a letter; the sign denotes normal (+) or reversed (—) polarity. *gc* = FOD of the *G. conomiozea* group; *5* = FOD of *G. menardii* form 5.

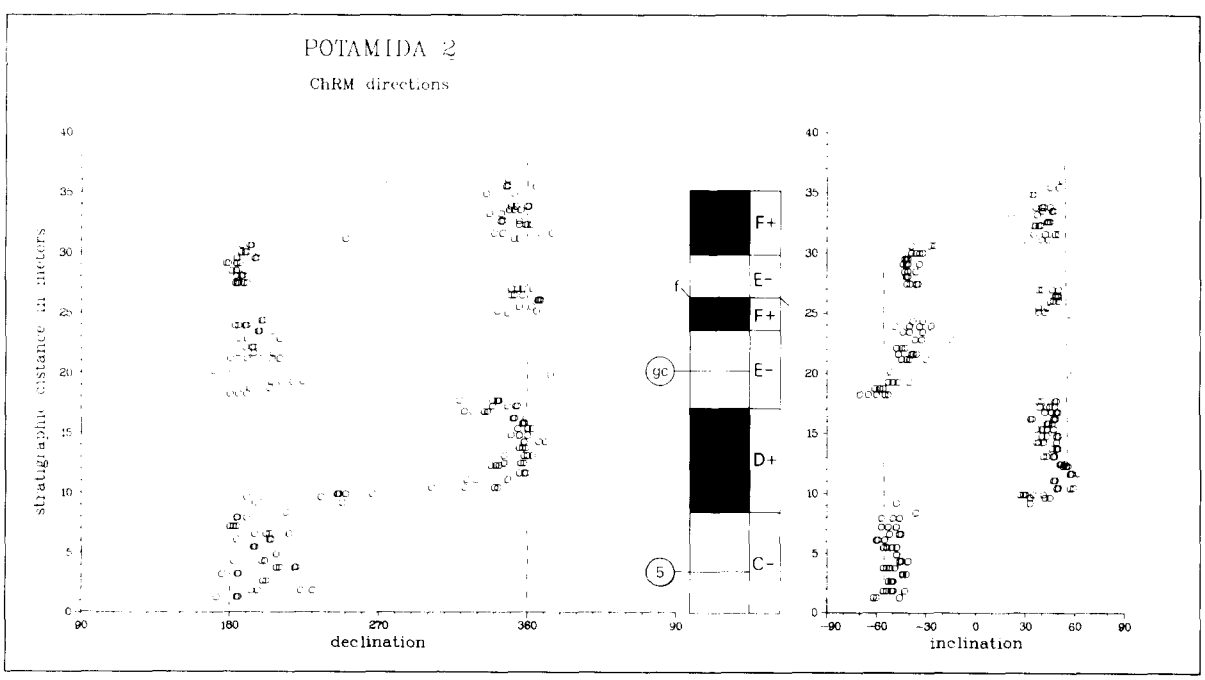

Fig. 7. Declination and inclination of ChRM in section Potamida 2. Doubling of polarity zones E— and F+ is caused by a fault (*f*). See also Fig. 6 caption.

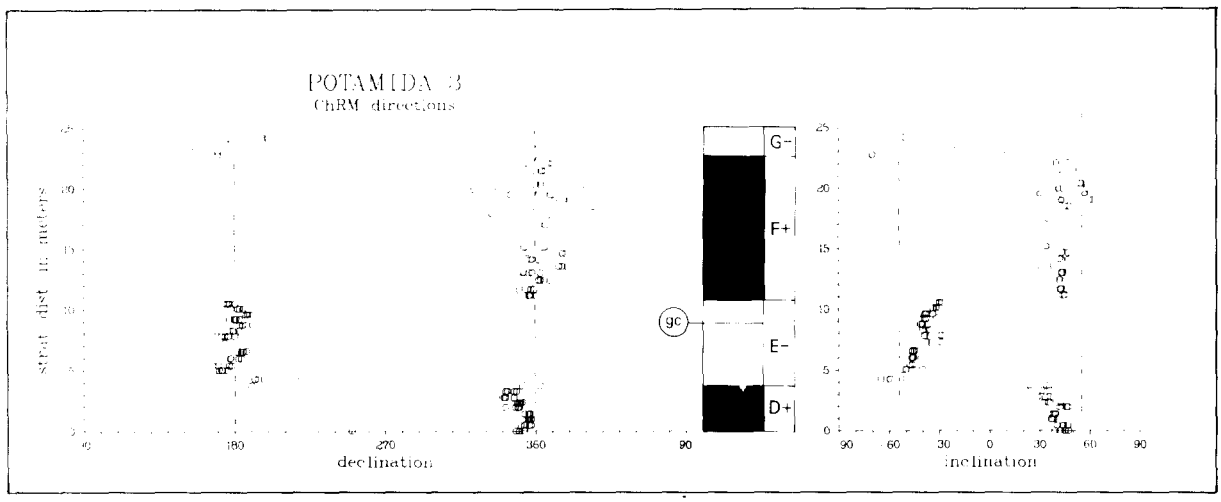

Fig. 8. Declination and inclination of ChRM in section Potamida 3. See also Fig. 6 caption.

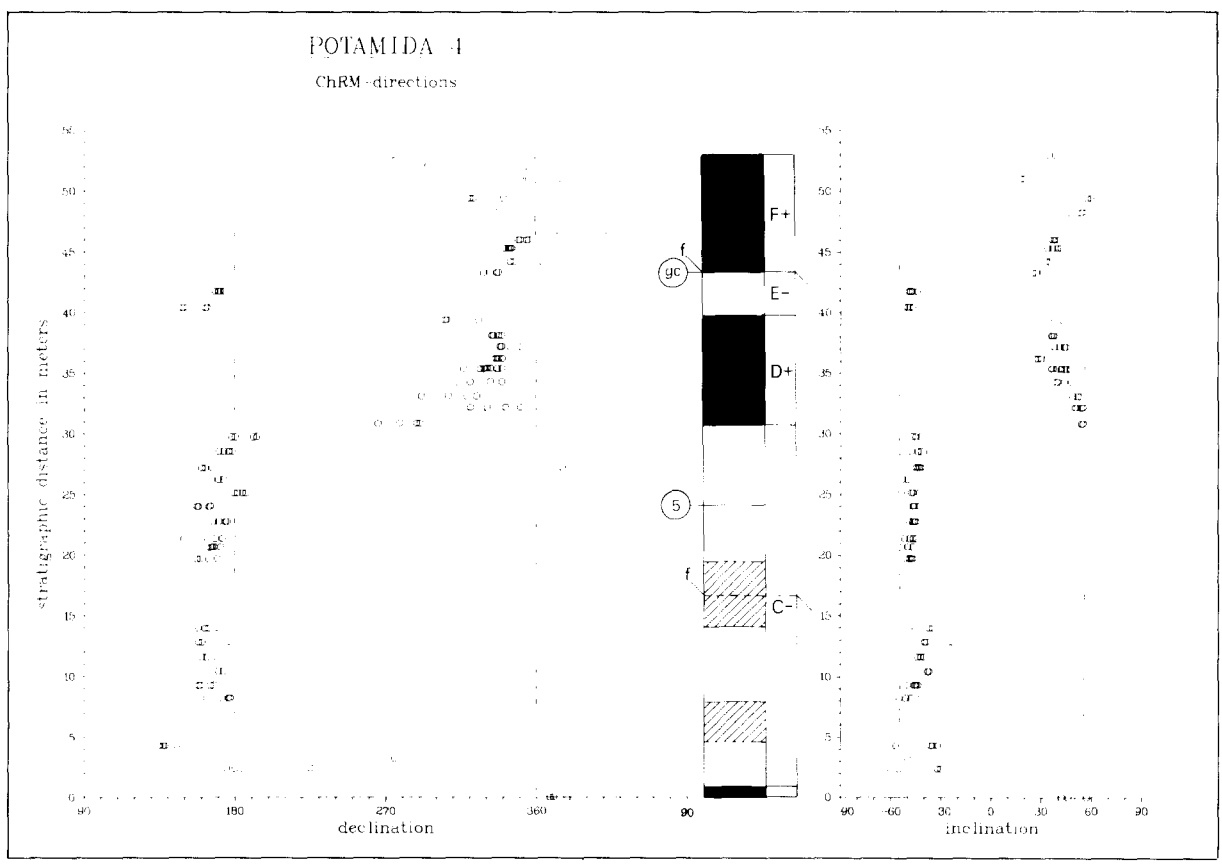

Fig. 9. Declination and inclination of ChRM in section Potamida 4. Hatched intervals refer to gaps in sample record; *f* indicates faults. See also Fig. 6 caption.

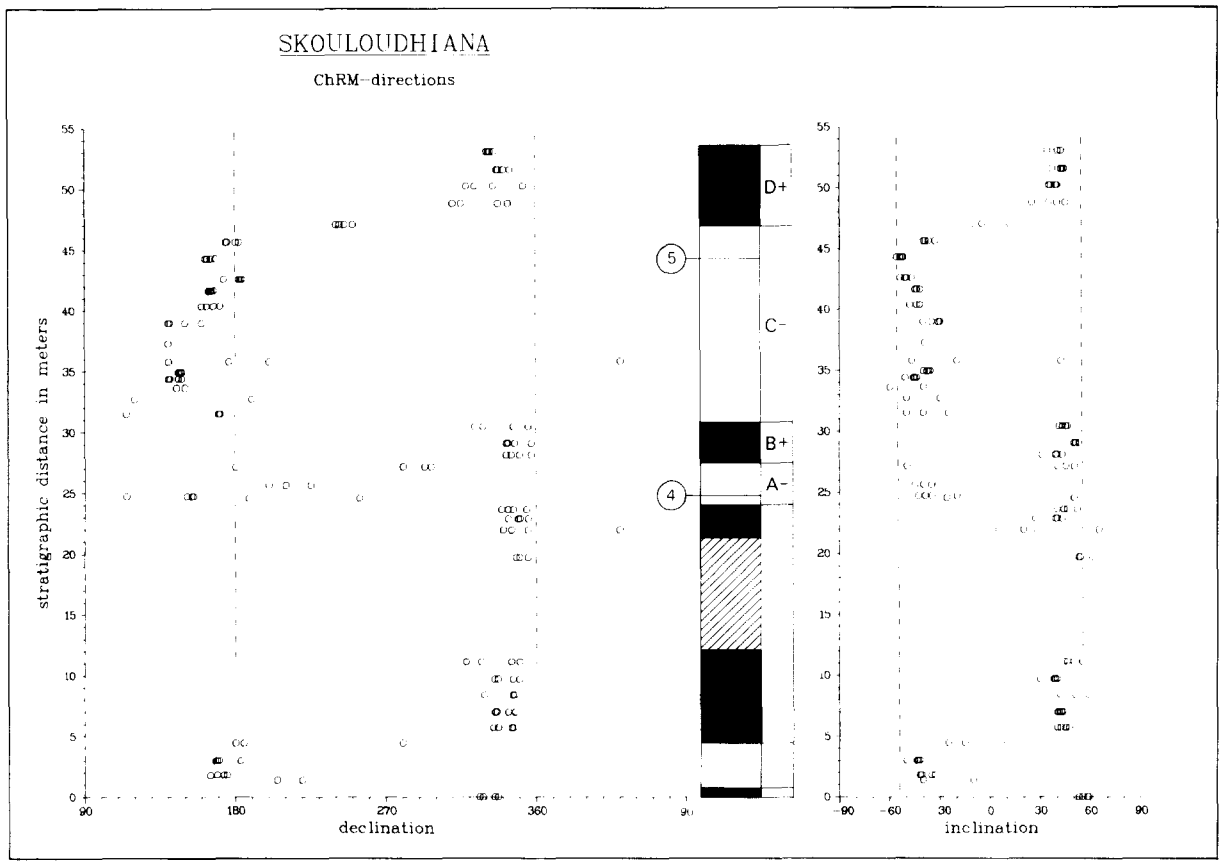

Fig. 10. Declination and inclination of ChRM in section Skouloudhiana. Hatched interval represents gap in sample record; *4* = LOD of *G. menardii* form 4. See also Fig. 6 caption.

B+ and A— are well defined. The long, covered interval below polarity zone A— means that there are possibly more polarity reversals present than the ones recorded in the lower part of section Skouloudhiana.

Some nine polarity reversals were recorded in section Kastelli in central Crete (Fig. 11). Biostratigraphically as well as magnetostratigraphically, section Kastelli can be clearly correlated with the western Cretan sections and allows the polarity zones in section Kastelli to be labelled in terms of the western Cretan polarity succession. As shown in Fig. 11, polarity zones A— through G— are recognizable in this section. As holds true for western Crete, the sediments overlying the Kastelli section are not suitable for paleomagnetic analysis.

Magnetobiostratigraphy for the Upper Miocene of Crete

Fig. 12 shows the position of the five western Cretan sections relative to selected polarity reversal horizons. When corrected for the small fault in the upper part of section Potamida 2 (Langereis, 1979; Drooger et al., 1979b) the polarity reversal sequence of this section correlates excellently with those in sections Potamida 1 and 3. Also corrected for faulting are the upper and lower part of section Potamida 4.

In sections Potamida 1 and 2 the FOD of the *Globorotalia conomiozea* group is recorded in the middle and in section Potamida 3 in the upper part of polarity zone E—. The anomalous position of the FOD of the *G.*

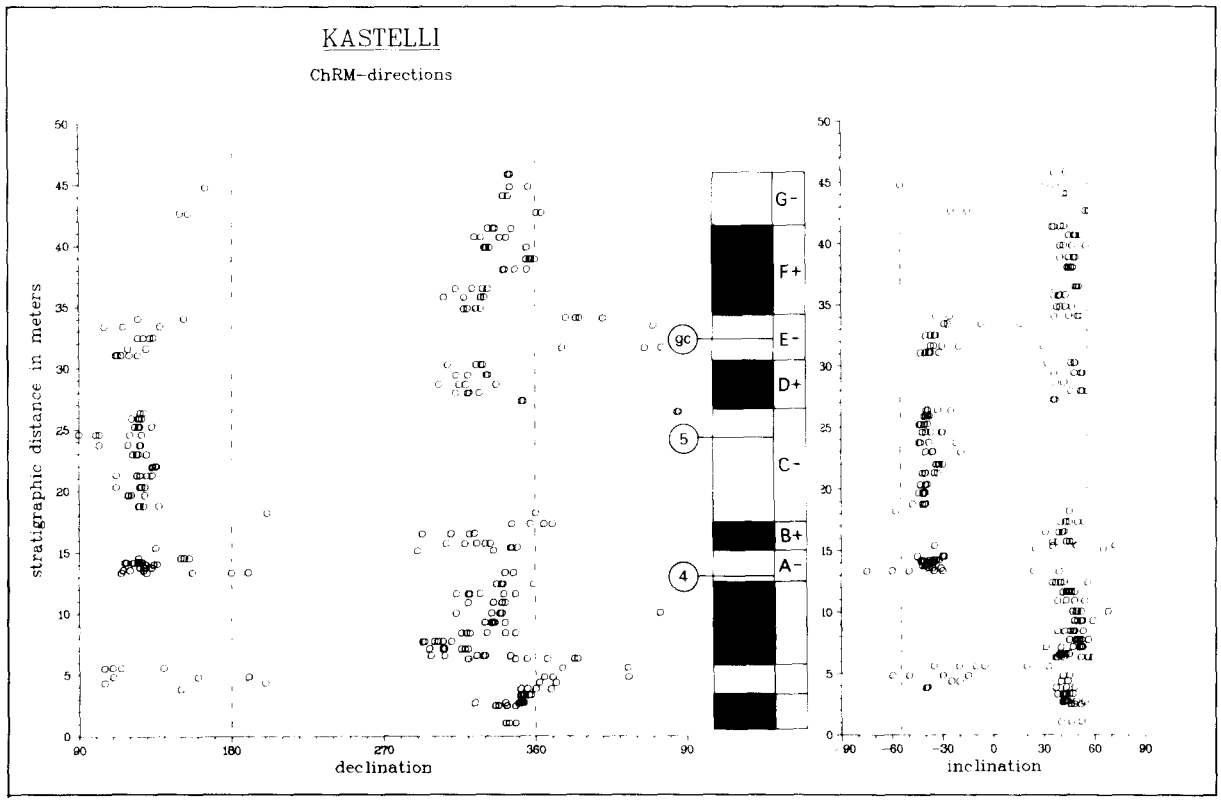

Fig. 11. Declination and inclination of ChRM in section Kastelli. See also Fig. 6 and Fig. 10 captions.

conomiozea group at the boundary of polarity zones E— and F+ in section Potamida 4 is related to a fault and illustrates that if a biohorizon coincides with a "polarity reversal horizon", a hiatus or fault must be taken into consideration.

The entry of *Globorotalia menardii* form 5 occurs in polarity zone C— of sections Potamida 1, 2 and 4 and of section Skouloudhiana (Fig. 12). The sudden and instantaneous re-appearance of sinistrally keeled globorotaliids above the FOD of *G. menardii* form 5 is recorded in polarity zone D+ of sections Potamida 1 and 3 (Fig. 12). Their absence in the other sections is ascribed to the (paleontologic) sample distance being a three to fourfold of that in sections Potamida 1 and 3. The LOD of *G. menardii* form 4 is recorded only in section Skouloudhiana and falls within polarity zone A—.

On the basis of the polarity reversal sequences of the five overlapping western Cretan sections a composite polarity stratigraphy is constructed in such a way that the lengths of the polarity zones are normalized to a uniform accumulation rate. Sections Potamida 1, 2 and 3 have polarity zone E— in common, the thickness of which is uniform. The same holds for polarity zone D+ in sections Potamida 1, 2 and 4, suggesting an equal accumulation rate in all four sections. Therefore the lengths of the upper three polarity zones of the composite column correspond to their actual measured lengths in sections Potamida 1 to 4.

The actual length of the long polarity zone C— is unknown in section Potamida 1 and uncertain in section Potamida 4. Section Skouloudhiana is the only section in which the length of this zone can be determined. The length, however, is notably shorter than the minimum length of this zone in section Potamida 1. This indicates that the average accumulation rate in section Skouloudhiana

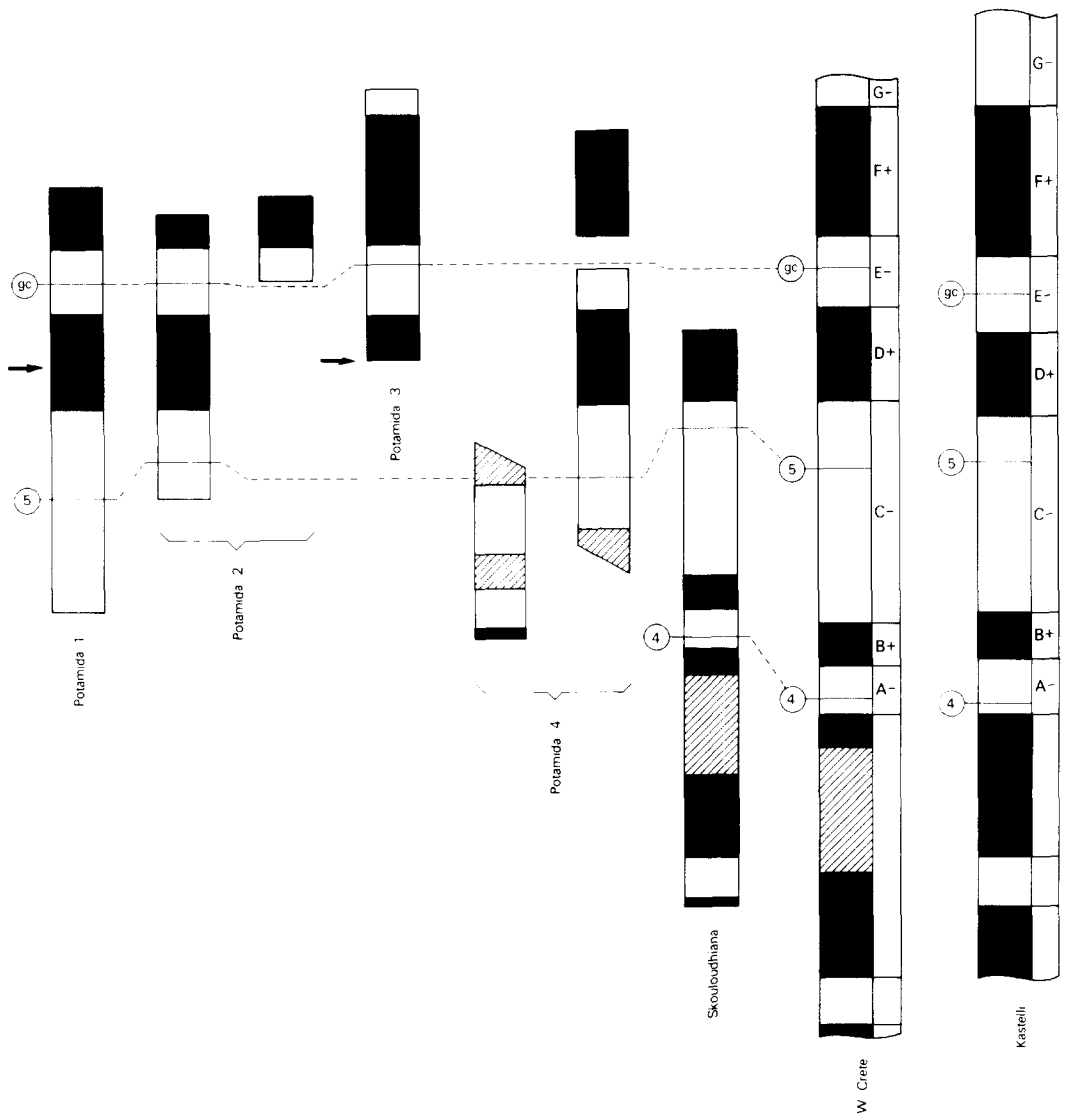

Fig. 12. Position of five western Cretan sections relative to selected polarity reversal horizons. Sections Potamida 2 and 4 have been corrected for faulting. The composite polarity stratigraphy for western Crete is given in the second column from the right. For the composite column the lengths of the polarity zones of section Skouloudhiana have been normalized to the average sedimentation rate of the Potamida sections. The column furthest to the right represents the succession of polarity zones in section Kastelli in central Crete. The lengths of the polarity zones of section Kastelli are adjusted to the average accumulation rate of the composite column of western Crete. See also Fig. 2 caption.

has been lower than in section Potamida 1. Therefore, polarity zone C— in Skouloudhiana must be "stretched" at least by a factor of 1.2 so that it is adjusted to the accumulation rate of the Potamida sections. If polarity zone D+ in section Skouloudhiana is adjusted to this accumulation rate, its length must be multiplied by at most a factor of 1.3. The average correction factor used here to normalize the length of the polarity zone C— in section Skouloudhiana is therefore fixed at 1.25. The same accumulation rate correction has been applied to the other polarity zones.

As shown in Fig. 12 the upper six polarity

zones of section Kastelli correlate excellently with the upper six polarity zones of the composite section of western Crete. The same holds for the position of the various biohorizons relative to the polarity reversal sequence. Correlation between the polarity patterns below the succession of six polarity zones is doubtful due to the non-exposed interval in western Crete. The total thickness of polarity zones A— through F+ amounts to 56.6 metres for the composite column in western Crete and 29 m for section Kastelli in central Crete, indicating that the average accumulation rate in the latter section has been a factor 1.95 less. In Fig. 12 the polarity zones of section Kastelli are "stretched" by the same factor of 1.95 in order to facilitate comparison with the composite column in western Crete.

In general, the relative lengths of the successive polarity zones in central Crete compare well with those in western Crete, suggesting that the accumulation rate in section Kastelli did not vary greatly or in the same way as in western Crete. An odd coincidence is that all but one of the biohorizons occur in the reversed polarity zones. Minor variations in the position of biohorizons relative to the polarity patterns are believed to have been caused by differences in the distance between samples, by minor fluctuations in the accumulation rate and/or by minor faults.

Correlation with the magnetic polarity time-scale

The next important step is to correlate the Cretan succession of six polarity zones with the magnetic polarity time-scale of Lowrie and Alvarez (1981).

For a correct correlation an undisturbed magnetic signal is essential, i.e., doubling or lacking of polarity zones may lead to erroneous conclusions. Therefore, the possibility of faults is considered carefully and whenever substantiated they are indicated (Figs. 6—11) and corrected for (Fig. 12). Moreover, employing an accumulation rate based on the average duration of 0.2 Ma for Upper Miocene polarity zones gives a magnetostratigraphic resolution of 10,000—25,000 years in western Crete and of 30,000—40,000 years in central Crete. Since the minimum duration of Late Miocene polarity zones is about 0.05 Ma, the high-resolution signal excludes the possibility of missing polarity (sub)zones.

The uniform lithology of massive clays and stable faunal/floral patterns (Drooger et al., 1979a) suggest furthermore a continuous accumulation at a more or less constant rate. Additional evidence for a fairly constant accumulation rate is provided by the uniform grain size distribution and composition of magnetic minerals inferred from the patterns of rock-magnetic properties (Langereis, 1984). Therefore, differences in relative lengths of the Cretan polarity zones supposedly closely reflect differences in duration of polarity chronozones.

The reliable and detailed magnetostratigraphy, however, appears not to be sufficient in itself to establish a conclusive correlation between the Cretan polarity sequence and the magnetic polarity time-scale. For instance, a computer run by which the Cretan polarity sequences are compared statistically with every possible sequence of six polarity zones over the last 15 Ma yields three significant correlations with corresponding ages for the FOD of the *Globorotalia conomiozea* group of 3.1, 5.6 and 11.7 Ma (Fig. 13). Hence, radiometric control on the Cretan polarity stratigraphy is a necessary addition for determining the correct correlation. In this case, indirect radiometric control is provided by the reported age-range of 6.0—7.0 Ma of the Mediterranean FOD of *Globorotalia conomiozea* (Van Couvering et al., 1976; Arias et al., 1976) which suffices to correlate the Cretan polarity sequence with chronozones 5 (anomaly 3A) and 6, by which the FOD of the *G. conomiozea* group is conclusively fixed at 5.6 Ma (Fig. 15).

The Blind River section in New Zealand contains the evolutionary appearance level of *Globorotalia conomiozea* and is tied to a detailed polarity reversal sequence (Kennett

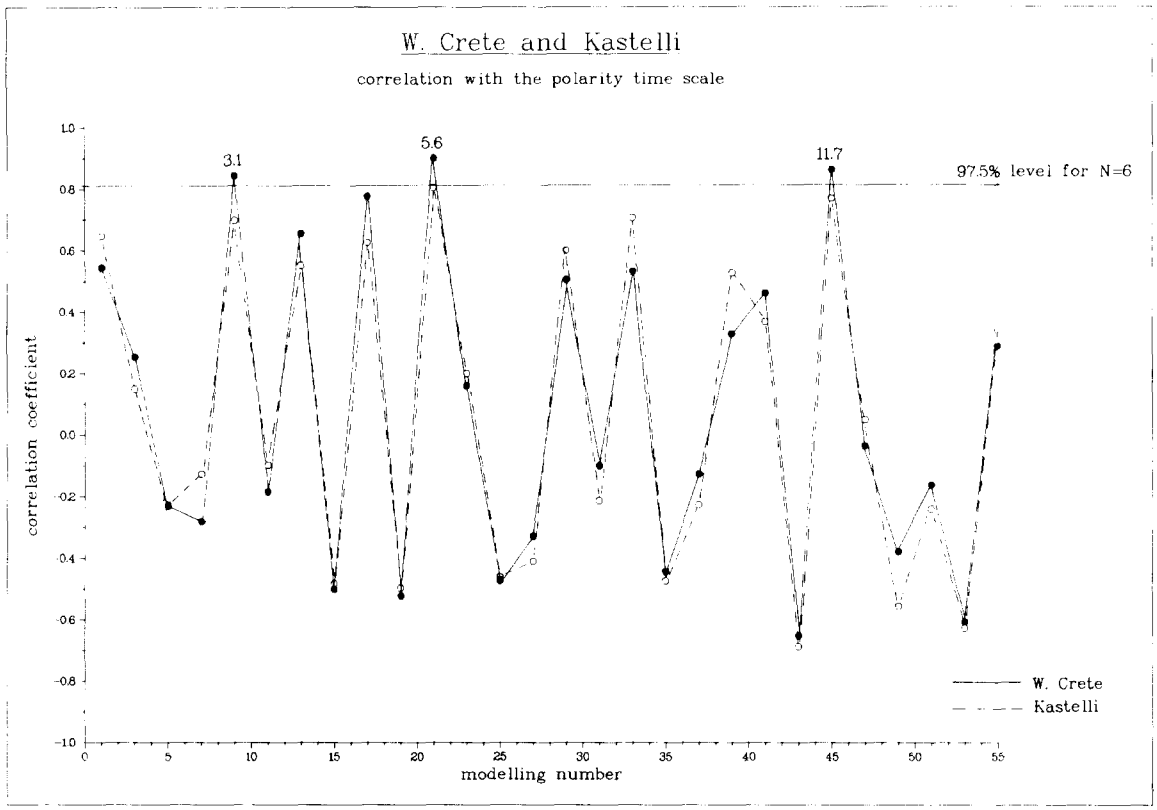

Fig. 13. Correlation coefficients between the pattern of lengths of polarity zones A— through F+ of the western Cretan composite section (solid line) and of the Kastelli section (dashed line) and the pattern of time-duration of each succession of six polarity zones between recent and 15.1 Ma of the magnetic polarity time-scale. For the correlations that show highest coefficients for both Cretan sequences together we give the corresponding ages of the FOD of the *G. conomiozea* group.

and Watkins, 1974). Comparing the polarity sequence of this section with every possible sequence of eight polarity zones over the last 15 Ma, yields the same three correlations with corresponding ages for the first evolutionary appearance level of *Globorotalia conomiozea* of 3.5, 6.0 and 12.2 Ma (Fig. 14). The age of 6.0 Ma has the highest correlation coefficient and agrees extremely well with the revised age determination of 6.1 ± 0.1 Ma reported by Loutit and Kennett (1979).

Polarity chronozones and age of the FOD of the *G. conomiozea* group

The identification of polarity chronozones 5 and 6 in the Upper Miocene of Crete with a corresponding age of 5.6 Ma for the FOD of the *Globorotalia conomiozea* group is an unexpected result and differs appreciably from the results of earlier attempts to date this biohorizon. Polarity sequences from supposedly time-equivalent sediments in the Tortonian type section (Rio Mazzapiedi) and in the Santerno section (northern Italy) have been investigated by Nagakawa et al. (1974, 1975). According to the interpretation of these authors the higher part of the Tortonian type section (Rio Mazzapiedi), sampled up to level 13 of Cita et al. (1965), would belong to polarity chronozone 8 and to the basal part of chronozone 7. This would imply that the FOD of *Globorotalia conomiozea*, reported by D'Onofrio et al. (1975) from a level slightly below level 13 of Cita et al. (1965), would occur approximately at the boundary

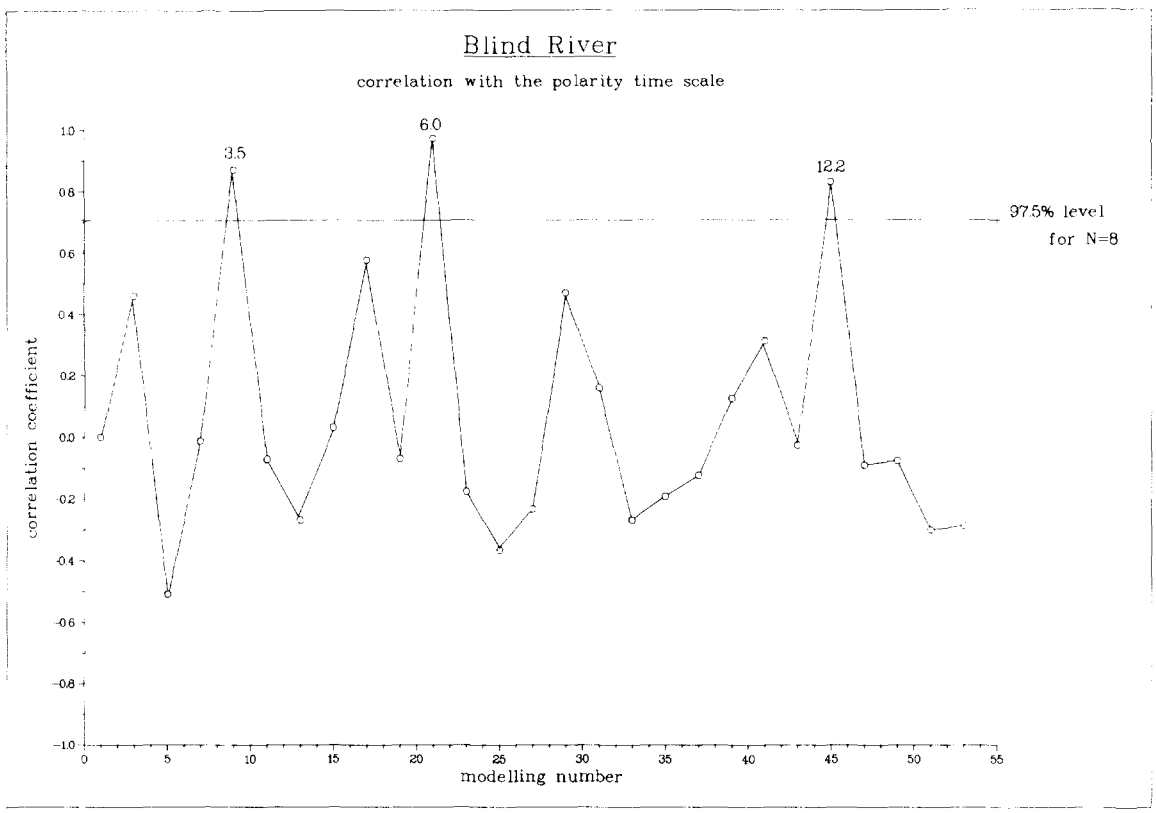

Fig. 14. Correlation coefficients between the pattern of lengths of eight polarity zones in the New Zealand Blind River section (Kennett and Watkins, 1974) and the pattern of time-duration of each succession of eight polarity zones between Recent and 15.1 Ma of the magnetic polarity time-scale. For the significant correlations we give the corresponding age of the evolutionary appearance of *G. conomiozea*.

of polarity chronozones 8 and 7 with a corresponding age of 7.4 Ma, according to the magnetic polarity time-scale of Lowrie and Alvarez (1981). In this case *Globorotalia conomiozea* types would arrive almost 2.0 Ma later in Crete than in Italy. As the sudden spreading of the *Globorotalia conomiozea* group most probably represents a migrational event (Zachariasse, 1979a, b; Wernli, 1980), an intra-Mediterranean time-lag of such an extent seems highly improbable. Another objection to calibrating the FOD of the *Globorotalia conomiozea* group to polarity chronozone 8 is that the non-evolutionary beginning of *G. conomiozea* morphotypes in the Mediterranean would amply antedate their evolutionary appearance in the Pacific (Loutit and Kennett, 1979). This latter argument, however, may be invalid if Scott (1980) is right that the Mediterranean *Globorotalia conomiozea* group is not related to the New Zealand taxon.

Radiometric ages for the FOD of *Globorotalia conomiozea* (Van Couvering et al., 1976; Arias et al., 1976) indicate that this biohorizon is definitely younger than is suggested by calibrating this event close to the boundary of polarity chronozones 8 and 7.

All evidence together indicates that the polarity reversal sequences measured by Nagakawa et al. (1974, 1975) in Tortonian/Messinian transitional strata of northern Italy are incorrectly assigned to polarity chronozones 8 and 7. Evidently, these polarity sequences represent a younger magnetic signal.

Adhering to an age of 5.6 Ma for the FOD of the *Globorotalia conomiozea* group in the Mediterranean, however, does not match with

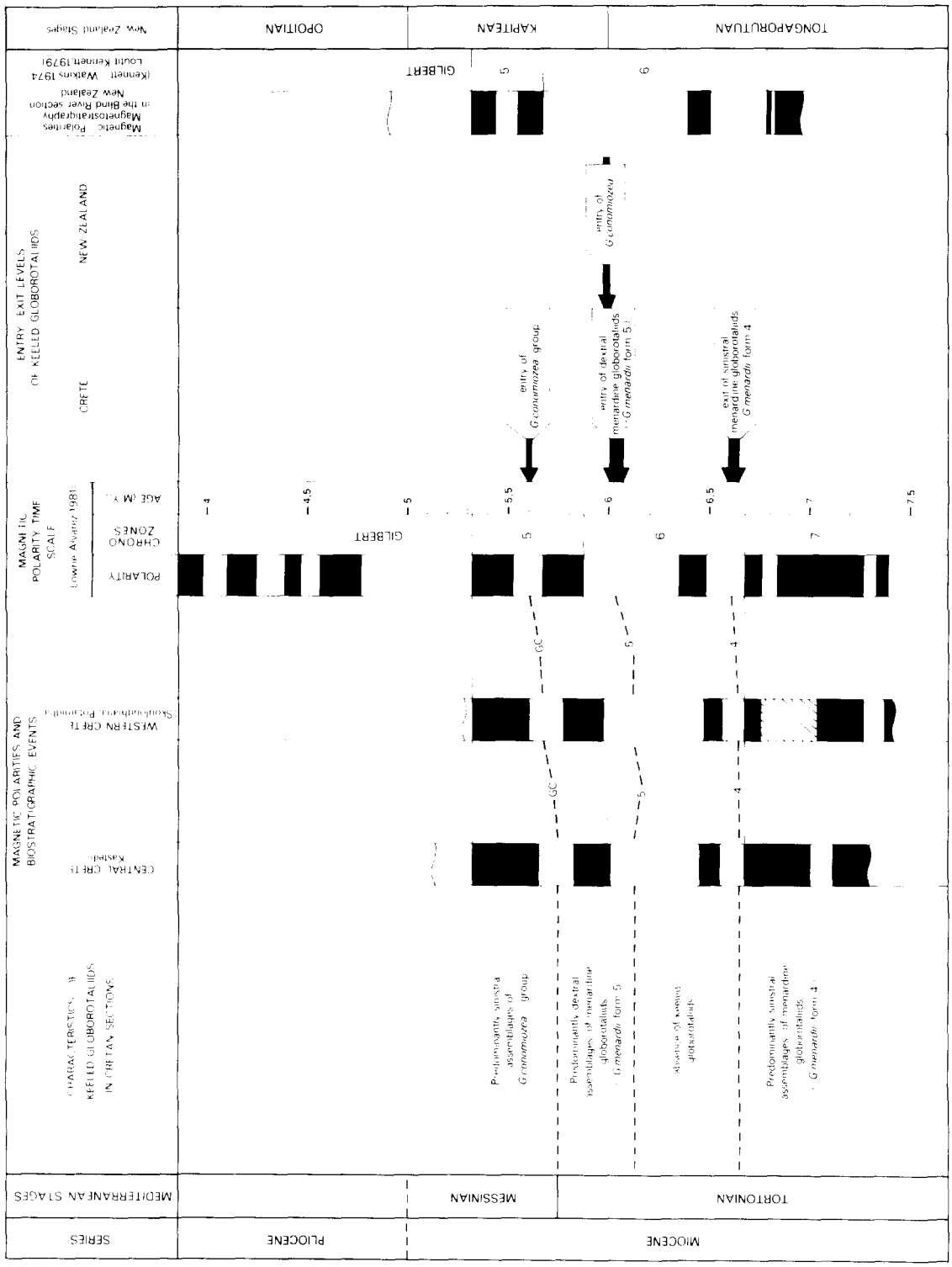

Fig. 15. Late Miocene biostratigraphic events, magnetic polarity zones and chronostratigraphic units in the Mediterranean and in New Zealand and their calibration to the magnetic polarity time-scale.

the reported age-range of 6.0—7.0 Ma for the FOD of *G. conomiozea* (Ryan et al., 1974; Van Couvering et al., 1976; Arias et al., 1976).

Radiometric ages most directly related to the FOD of the *Globorotalia conomiozea* group are provided by Arias et al. (1976). In the Izarorene section in Morocco these authors dated several tuff layers from an interval slightly below the FOD of *Globorotalia conomiozea*. Radiometric datings thus provide a maximum age for this biostratigraphic event. However, the range of radiometric ages for individual tuff layers is very large, varying between 5.6 ± 0.3 (sic) and 7.1 ± 0.4 Ma for the K/Ar datings and between 6.3 ± 1.1 and 6.8 ± 0.6 Ma for the fission track datings. Therefore a maximum age for the FOD of *Globorotalia conomiozea* in Morocco, ranging from 5.6 ± 0.3 to 7.1 ± 0.4 Ma, is not necessarily in conflict with an inferred age of 5.6 Ma for the FOD of the *G. conomiozea* group in Crete.

In southern Spain marine sediments with intercalated volcanic lava flows, dated at 6.9 Ma, contain planktonic foraminiferal associations which predate the FOD of *Globorotalia conomiozea* and which are of presumably Late Tortonian Age (Van Couvering et al., 1976). These marine sediments are overlain by continental deposits containing a mammalian fauna (Librille fauna) correlatable with the mammalian fauna level VI at Crevillente, which in turn correlates with marine sediments containing *Globorotalia conomiozea* (De Bruijn et al., 1975). Thus the FOD of *G. conomiozea* can only indirectly be calibrated to this radiometric age of 6.9 Ma, which gives at best a maximum age determination for this event.

The age of 6.3 Ma for the FOD of *Globorotalia conomiozea* in the Mediterranean, given by Ryan et al. (1974), is based on the reinterpretation of the paleomagnetic data from the Blind River section in New Zealand (Kennett and Watkins, 1974) and on the assumption that the New Zealand FOD of *G. conomiozea* is time-equivalent with the Mediterranean FOD of *G. conomiozea*. Although the reinterpreted magnetic correlation for the Blind River is generally accepted, Ryan et al. did not place the FOD of *Globorotalia conomiozea* in accordance with the original data of Kennett and Watkins (1974). If it were positioned correctly, the FOD of *Globorotalia conomiozea* would occur in the younger reversed interval of polarity chronozone 6 with an extrapolated age of ca. 6.1 Ma (Loutit and Kennett, 1979; Fig. 15).

The results of the present study demonstrate that the diachrony between the New Zealand FOD of *Globorotalia conomiozea* and the FOD of the *G. conomiozea* group in the Mediterranean is 0.4 Ma. The diachrony between both biohorizons is explicable in view of the different nature of their corresponding events, the one in New Zealand being evolutionary and the one in the Mediterranean being migrational.

Age of the Tortonian/Messinian boundary and the main evaporitic phase

Unfortunately no reliable magnetostratigraphic data are available to determine the degree of synchrony of the FOD of the *Globorotalia conomiozea* group in the Mediterranean. Upper Miocene sequences in the Caltanisetta Basin (Sicily), including the recently proposed boundary stratotype section for the Tortonian/Messinian boundary (Colalongo et al., 1979) appear to have been completely remagnetized and show only recent, normal polarities (Langereis, 1984).

Evidence for the supposedly time-equivalence of the Mediterranean FOD of the *Globorotalia conomiozea* group, however, is recently provided by a refined calcareous nannoplankton stratigraphy (Theodoridis, 1983): both in Crete and in Sicily the FOD of the *G. conomiozea* group nearly coincides with the entry level of *Reticulofenestra rotaria*. In combination with the observation that the FOD of the *Globorotalia conomiozea* group in the Tortonian/Messinian boundary stratotype section (Zachariasse and Spaak, 1983) coincides with the level proposed as the physical reference point for the Tortonian/Messinian boundary (Colalongo et al., 1979),

an age of 5.6 Ma is provided for this boundary.

Since the youngest sediments incorporated in our study reach into the Gilbert chronozone (Fig. 15) and antedate the abrupt coiling change in *Neogloboquadrina acostaensis*, the latter event must be younger than the base of the Gilbert chronozone whose age is fixed at 5.3 Ma (Lowrie and Alvarez, 1981). In the Mediterranean the abrupt coiling change in neogloboquadrinids occurs at a level slightly below the main evaporitic phase (Zachariasse, 1975; Colalongo et al., 1979), which means that the Messinian evaporitic body has a lower age limit of about 5.3 Ma. Since an abrupt coiling change in neogloboquadrinids is also documented in the North Atlantic record (e.g. Berggren, 1972; Poore, 1979), this event could form an important link in Late Miocene biostratigraphic correlations between the Mediterranean and the temperate North Atlantic. The sudden introduction of dextrally coiled neogloboquadrinids in the Mediterranean is linked with an equatorwards migration of coiling provinces on the North Atlantic (Van der Zwaan, 1982; Zachariasse and Spaak, 1983), The coiling change in *Neogloboquadrina pachyderma* reported by de Meuter and Laga (1970) from the Kattendijk Sands (Belgium) may be a reflection of the same biogeographic change in the North Sea Basin. If so, then the Kattendijk Sands are of Late Miocene age and were deposited during the time the Mediterranean entered the main evaporitic phase.

The age of the Miocene/Pliocene boundary is commonly fixed at about 5.0 Ma and is based on the calibration of multiple biostratigraphic criteria to the magnetic polarity timescale (Berggren, 1973; Cita and Gartner, 1973; Berggren and Van Couvering, 1974), all of which are at best of questionable usage in the Mediterranean. Commonly, the recognition of the base of the Mediterranean Pliocene is based on the sedimentary expression of the post-Messinian flooding and must certainly be older than 4.4 ± 0.2 Ma (Benda et al., 1979), and is probably older than 4.7 Ma according to the radiometric age of the supposedly Lower Pliocene Orciatico trachyte in Tuscany (Selli, 1970). Whatever the precise age for the base of the Pliocene in the Mediterranean may be, it is evident that the new age of 5.6 Ma for the Tortonian/Messinian boundary severely reduces the time-span of the Messinian.

Adopting the age of 5.0 Ma for the Miocene/Pliocene boundary would imply that the evaporites and post-evaporitic Lago Mare sediments were deposited in some 300,000 years. Given the thickness of more than 1000 m for the Messinian evaporitic body in the central parts of the Mediterranean basins (e.g. Leenhardt, 1973; Selli, 1973; Mulder, 1973; Hsü et al., 1977) the evaporites must have accumulated at rates of more than 3 m per 1000 years.

Accumulation rates of this order of magnitude are known for anhydrites and halites precipitated in the central parts of Permian concentration basins (Richter-Bernburg, 1953) as well as for gypsum growth in recent salinas (Dronkert, 1977).

The extremely short time-span in which thick evaporitic bodies could accumulate in the central parts of the Mediterranean basins concurs better with a deep-water origin for the evaporites (i.e. precipitation in concentration basins with a heavy brine reflux circulation) than with an origin by evaporation in a recurrent desiccated basin (Hsü et al., 1973).

Acknowledgements

P. Dankers provided useful assistance in the early phases of this work. C.W. Drooger and J.E. Meulenkamp are thanked for critically reading the manuscript. Special thanks are due to P.J. Verplak for his pleasant company in the field and for his invaluable help in the laboratory. P. de Boer made helpful suggestions concerning the statistics. This study was supported by the Netherlands Organisation for the Advancement of Pure Science (ZWO).

References

Arias, C., Bigazzi, G., Bonadonna, F.P., Morlotti, E., Radicati di Brozolo, F., Rio, D., Torelli, L., Brigatti, M.F., Giuliani, O. and Tirelli, G., 1976. Chronostratigraphy of the Izarorene section in the Melilla Basin (northeastern Morocco). Boll. Soc. Geol. Ital., 95: 1681—1694.

Benda, L., Jonkers, H.A., Meulenkamp, J.E. and Steffens, P., 1979. Biostratigraphic correlations in the Eastern Mediterranean Neogene, 4. Marine microfossils, sporomorphs and radiometric data from the Lower Pliocene of Ag. Thomas, Aegina, Greece. Newsl. Strat., 8(1): 61—69.

Berggren, W.A., 1972. Cenozoic biostratigraphy and paleobiogeography of the North Atlantic. Initial Reports of the Deep Sea Drilling Project, 12: 965—1001.

Berggren, W.A., 1973. The Pliocene time-scale: calibration of planktonic foraminiferal and calcareous nannoplankton zones. Nature, 243: 391—397.

Berggren, W.A. and Van Couvering, J.A., 1974. The Late Neogene: biostratigraphy, geochronology and paleoclimatology of the last 15 million years in marine and continental sequences. Palaeogeogr., Palaeoclimatol., Palaeoecol., 16(1—2): 1—216.

Cita, M.B., Premoli Silva, I. and Rossi, R., 1965. Foraminiferi planctonici del Tortoniano-tipo. Riv. Ital. Paleontol., 71(1): 217—308.

Cita, M.B. and Gartner, S., 1973. The stratotype Zanclean foraminiferal and nannofossil biostratigraphy. Riv. Ital. Paleontol., 79(4): 503—558.

Colalongo, M.L., Di Grande, A., D'Onofrio, S., Gianelli, L., Iaccarino, S., Mazzei, R., Poppi Brigatti, M.F., Romeo, M., Rossi, A. and Salvatorini, G., 1979. A proposal for the Tortonian/Messinian boundary. Ann. Géol. Pays Hellén., Tome hors série, 1979, fasc. I, 285—294. VIIth International Congress on Mediterranean Neogene, Athens, 1979.

De Bruijn, H., Mein, P., Montenat, C. and Van der Weerd, A., 1975. Correlations entres les gisements des rongeurs et les formations marines du Miocene terminal d'Espagne méridionale (Prov. d'Alicante et de Murcia). Proc. Kon. Nederl. Akad. Wet., Ser. B, 78(4): 282—313.

De Meuter, F.J.C. and Laga, P.G.H., 1970. Coiling ratios and other variations of *Globigerina pachyderma* (EHRENBERG, 1861) and the stratigraphical significance in the Neogene deposits of the Antwerpen area (Belgium). Bull. Soc. Belge Géol., Paléontol., Hydrol., 79(2): 175—184.

D'Onofrio, S., Gianelli, L., Iaccarino, S., Morlotti, E., Romeo, E., Salvatorini, G., Sampo, M. and Sprovieri, R., 1975. Planktonic foraminifera of the Upper Miocene from some Italian sections and the problem of the lower boundary of the Messinian. Boll. Soc. Paleontol. Ital., 14(2): 177—196.

Dronkert, H., 1977. A preliminary note on a recent sabkha deposit in S. Spain. Inst. Invest. Geol. Diput, Prov. Univ. Barcelona, 32: 153—166.

Drooger, C.W., Meulenkamp, J.E., Langereis, C.G., Wonders, A.A.H., Van der Zwaan, G.J., Drooger, M.M., Raju, D.S.N., Doeven, P.H., Zachariasse, W.J., Schmidt, R.R. and Zijderveld, J.D.A., 1979a. Problems of detailed biostratigraphic and magnetostratigraphic correlation in the Potamidha and Apostoli sections in the Cretan Neogene. Utrecht Micropaleontol, Bull., 21.

Drooger, C.W., Langereis, C.G., Meulenkamp, J.E. and Zijderveld, J.D.A., 1979b. The correlation of both Potamidha sections: retrospect and final conclusions. Utrecht Micropaleontol. Bull., 21: 215—222.

Freudenthal, Th., 1969. Stratigraphy of Neogene deposits in the Khania Province, Crete, with special reference to foraminifera of the family Planorbulinidae and the genus *Heterostegina*. Utrecht Micropaleontol. Bull., 1.

Hsü, K.J., Cita, M.B. and Ryan, W.B.F., 1973. The origin of the Mediterranean evaporites. Initial Reports of the Deep Sea Drilling Project, 13: 1203—1231.

Hsü, K.J., Montadert, L., Bernoulli, D., Cita, M.B., Erickson, A., Garrison, R.E., Kidd, R.B., Melieres, F., Muller, C. and Wright, R., 1977. History of the Mediterranean salinity crisis. Nature, 267: 399—403.

Kennett, J.P. and Watkins, N.D., 1974. Late Miocene—Early Pliocene paleomagnetic stratigraphy, paleoclimatology, and biostratigraphy in New Zealand. Geol. Soc. Am. Bull., 85: 1385—1398.

King, R.F., 1955. Remanent magnetism of artificially deposited sediments. Mon. Notic. R. Astron. Soc., Geophys. Suppl., 7: 115—134.

Langereis, C.G., 1979. An attempt to correlate two adjacent Tortonian marine clay sections in western Crete using magnetostratigraphic methods. Utrecht Micropaleontol. Bull., 21: 193—214.

Langereis, C.G., 1984. Late Miocene magnetostratigraphy in the Mediterranean. Geol. Ultraiectina, 34.

Langereis, C.G. and Meulenkamp, J.E., 1979. Comparison of two methods used to measure lithostratigraphical intervals in section Potamidha 1 and 2. Utrecht Micropaleontol. Bull., 21: 22—26.

Langereis, C.G. and Zijderveld, J.D.A., 1979. Magnetostratigraphy of two Tortonian marine clay sections in western Crete. Ann. Géol. Pays. Hellén., Tome hors série, 1979, fasc. II, 711—716. VIIth International Congress on Mediterranean Neogene, Athens, 1979.

Leenhardt, O., 1973. Distribution and thickness of the Messinian evaporites in the western Mediterranean. In: C.W. Drooger (Editor), Messinian Events in the Mediterranean. North-Holland Publ. Co., Amsterdam, pp. 39—43.

Loutit, T.S. and Kennett, J.P., 1979. Application of carbon isotope stratigraphy to Late Miocene shallow marine sediments, New Zealand. Science, 204: 392—397.

Lowrie, W. and Alvarez, W., 1981. One hundred million years of geomagnetic polarity history. Geology, 9: 392—397.

Meulenkamp, J.E., 1969. Stratigraphy of Neogene deposits in the Rethymnon province, Crete, with special reference to the phylogeny of uniserial *Uvigerina* from the Mediterranean region. Utrecht Micropaleontol. Bull., 2.

Meulenkamp, J.E., 1979a. Lithostratigraphy and relative chronostratigraphic position of the sections Apostoli and Potamidha 1 and 2. Utrecht Micropaleontol. Bull., 21: 9—21.

Meulenkamp, J.E., 1979b. Field guide to the Neogene of Crete. Publ. of the Dept. of Geol. and Pal., Univ. Athens, Series A, 32.

Meulenkamp, J.E., Jonkers, H.A. and Spaak, P., 1979. Late Miocene—Early Pliocene development of Crete. Proc. 6th Coll. Geol. Aegean Region, 1: 137—149.

Mulder, C.J., 1973. Tectonic framework and distribution of Miocene evaporites in the Mediterranean. In: C.W. Drooger (Editor), Messinian Events in the Mediterranean. North-Holland Publ. Co., Amsterdam, pp. 44—59.

Nagakawa, H., Niitsuma, N., Kitamura, N., Matoba, Y., Takayama, T. and Asano, K., 1974. Preliminary results on magnetostratigraphy of Neogene stage stratotype sections in Italy. Riv. Ital. Paleontol., 80(4): 615—630.

Nagakawa, N., Niitsuma, N., Kimura, K. and Sakai, T., 1975. Magnetic stratigraphy of Late Cenozoic stages in Italy and their correlatives in Japan. In: T. Saito and L.H. Burckle (Editors), Late Neogene Epoch Boundaries. Micropaleontol., Spec. Publ., 1: 64—74. (Micropaleontology Press, New York).

Poore, R.Z., 1979. Oligocene through Quaternary planktonic foraminiferal biostratigraphy of the North Atlantic. Initial Reports of the Deep Sea Drilling Project, 49: 447—517.

Richter-Bernburg, G., 1953. Über salinare Sedimentation. Z. Dtsch. Geol. Ges., 105: 593—645.

Ryan, W.B.F., Cita, M.B., Dreyfus Rawson, M., Burckle, L.H. and Saito, T., 1974. A paleomagnetic assignment of Neogene stage boundaries and the development of isochronous datum planes between the Mediterranean, the Pacific and Indian oceans in order to investigate the response of the world ocean to the Mediterranean salinity crisis. Riv. Ital. Paleontol., 80, 80(4): 631—688.

Schmidt, R.R., 1973. A calcareous nannoplankton zonation for the Upper Miocene—Pliocene deposits from the southern Aegean area with a comparison to Mediterranean stratotype localities. Proc. Kon. Nederl. Akad. Wet., Ser. B., 76: 287—310.

Scott, G.H., 1980. Upper Miocene biostratigraphy: does *Globorotalia conomiozea* occur in the Messinian? Rev. Esp. Micropal., 12(3): 489—506.

Selli, R., 1970. Report on the absolute age. CMNS Proc. IV Session, Bologna, 1967, G. Geol., 25(1): 51—59.

Selli, R., 1973. An outline of the Italian Messinian. In: C.W. Drooger (Editor), Messinian Events in the Mediterranean. North-Holland Publ. Co., Amsterdam, pp. 150—171.

Sissingh, W., 1972. Late Cenozoic ostracoda of the South Aegean Island arc. Utrecht Micropaleontol. Bull., 6.

Theodoridis, S.A., 1983. Miocene calcareous nannoplankton zonation and revision of the genera *Discoaster* and *Helicosphaera*. Utrecht Micropaleontol. Bull., 32. In press.

Tjalsma, R.C., 1971. Stratigraphy and foraminifera of the Neogene of the eastern Guadalquivir Basin (southern Spain), Utrecht Micropaleontol. Bull., 4.

Valente, J.-P., Laj, C., Sorel, D., Roy, S. and Valet, J.-P., 1982. Paleomagnetic results from Mio-Pliocene marine sedimentary series in Crete. Earth Planet. Sci. Lett., 57: 159—172.

Van Couvering, J.A., Berggren, W.A., Drake, R.E., Aguirre, E. and Curtis, G.H., 1976. The terminal Miocene Event, Marine Micropaleontol., 1: 263—286.

Van der Zwaan, G.J., 1982. Paleoecology of Late Miocene Mediterranean foraminifera. Utrecht Micropaleontol. Bull., 25.

Wernli, R., 1980. Le Messinien à *Globorotalia conomiozea* (foraminifère planctonique) de la côte méditerranéenne marocaine. Eclogae Geol. Helv., 73(1): 71—93.

Wilson, R.L., 1971. Dipole offset — The time average paleomagnetic field over the past 25 million years. Geophys. J., 22: 491—504.

Zachariasse, W.J., 1975. Planktonic foraminiferal biostratigraphy of the Late Neogene of Crete (Greece). Utrecht Micropaleontol. Bull., 11.

Zachariasse, W.J., 1979a. Planktonic foraminifera from Potamidha 1: taxonomic and phyletic aspects of keeled globorotaliids and some environmental estimates. Utrecht Micropaleontol. Bull., 21: 129—166.

Zachariasse, W.J., 1979b. The origin of *Globorotalia conomiozea* in the Mediterranean and the value of its entry level in biostratigraphic correlations. Ann. Géol. Pays Hellén., Tome hors série, 1979, fasc. III, 1281—1292. VIIth International Congress on Mediterranean Neogene, Athens, 1979.

Zachariasse, W.J. and Spaak, P., 1983. Middle Miocene to Pliocene paleoenvironmental reconstruction of the Mediterranean and adjacent Atlantic Ocean: planktonic foraminiferal record of southern Italy. Utrecht Micropaleontol. Bull., 30. In press.